**Biogeosciences
Discussions**

# Role of land surface processes and diffuse/direct radiation partitioning in simulating the European climate

**E. L. Davin and S. I. Seneviratne**

Institute for Atmospheric and Climate Science, ETH Zurich, Zürich, Switzerland

Correspondence to: E. L. Davin (edouard.davin@env.ethz.ch)

Title Page

| Abstract | Introduction |
| Conclusions | References |
| Tables | Figures |

|◄ | ►|

◄ | ►

Back | Close

Full Screen / Esc

Printer-friendly Version

Interactive Discussion

**COSMO-CLM**[2]

E. L. Davin and
S. I. Seneviratne

## Abstract

The influence of land processes and in particular of diffuse/direct radiation partitioning on surface fluxes and associated regional-scale climate feedbacks is investigated. ERA-40 driven simulations over Europe are performed using the COSMO-CLM² Regional Climate Model (RCM). Two alternative Land Surface Models (LSMs), a 2nd generation LSM (TERRA_ML) and a more advanced 3rd generation LSM (Community Land Model version 3.5), and two versions of the atmospheric component are tested, as well as a revised coupling procedure allowing for variations in diffuse/direct light partitioning at the surface, and their accounting by the land surface component.

Overall, the RCM performance for various variables (e.g., surface fluxes, temperature and precipitation) is improved when using the more advanced 3rd generation LSM. These improvements are of the same order of magnitude as those arising from a new version of the atmospheric component, demonstrating the benefit of using a realistic representation of land surface processes for regional climate simulations. Taking into account variability in diffuse/direct light partitioning at the surface further improves the model performance in terms of summer temperature variability at the monthly and daily time scales. Comparisons with observations show that the RCM realistically captures temporal variations in diffuse/direct light partitioning as well as the evapotranspiration sensitivity to these variations. Our results suggest that a modest but consistent fraction (up to 3 %) of the overall variability in summer temperature can be explained by variations in the diffuse to direct ratio.

## 1 Introduction

The physical, chemical and biological processes acting at the interface between the land surface and the atmosphere influence the Earth's climate at various spatiotemporal scales (e.g., Bonan, 2008; Seneviratne et al., 2010; Arneth et al., 2010). The important role of land-atmosphere interactions was already explicitly recognized during

the design of the first climate models, which conceptualized the exchanges of radiation, heat and water between the land and the atmosphere through relatively simple land surface parametrization (e.g., Manabe, 1969). Since then, Land Surface Models (LSMs) have been continuously improved, to a point where they can represent the linkages between energy, water and nutrients cycles within the terrestrial biosphere.

Current Regional Climate Models (RCMs), however, often do not fully reflect the latest advances in LSM development, which is more tightly linked to the development of global models. Indeed, the progress towards global Earth System Models (ESMs) explicitly representing climate-carbon cycle interactions have motivated the use of advanced, biogeochemistry-enabled LSMs within global climate models (Friedlingstein et al., 2006), while regional climate modelling studies have been comparatively more focused on atmospheric processes and often relied on much simpler LSMs (Giorgi, 2006).

However, recent efforts have pointed out the potential added value of integrating more comprehensive LSMs into RCMs. The coupling between RAMS (Regional Atmospheric Modelling System) and the CENTURY biogeochemistry model showed that the phenological cycle of vegetation can significantly affect water and energy fluxes and thus regional climate (Lu et al., 2001). RAMS was also coupled to the SiB (Simple Biosphere) model in order to simulate diurnal and synoptical variations in $CO_2$ fluxes and atmospheric $CO_2$ concentrations over North America (Denning et al., 2003; Wang et al., 2007). The coupling between RegCM3 (Regional Climate Model version 3) and CLM3 (Community Land Model version 3) improved the simulated characteristics of the monsoon over West Africa (Steiner et al., 2009). RegCM3 was also coupled to IBIS (Integrated Biosphere Simulator) which led to a better simulation of latent heat flux over North America, although biases were increased for surface temperature and sensible heat flux (Winter et al., 2009). Finally, in a coupling between WRF3 (Weather Research and Forecasting model version 3) and CLM3.5 (Community Land Model version 3.5), Subin et al. (2011) illustrated the usefulness of RCMs to study the impact of land cover change on climate at the regional scale.

**COSMO-CLM**[2]

E. L. Davin and
S. I. Seneviratne

Title Page

Abstract | Introduction

Conclusions | References

Tables | Figures

◄ | ►►

◄ | ►

Back | Close

Full Screen / Esc

Printer-friendly Version

Interactive Discussion

The COSMO-CLM model version 4.0 has been recently coupled to CLM3.5 in order to improve the representation of land surface processes in the context of regional climate simulations (Davin et al., 2011). In this new model configuration termed COSMO-CLM[2], CLM3.5 replaces TERRA_ML, the native LSM included in COSMO-CLM. When using CLM3.5 instead of TERRA_ML, Davin et al. (2011) found an overall improvement in the simulated climate over Europe, in particular for cloud cover, temperature and precipitation. This was due to a more realistic simulation of surface fluxes and more specifically a better partitioning between sensible and latent heat. However, important biases still remained in the model, such as a large underestimation of surface net shortwave radiation (Davin et al., 2011).

Here, we present an updated version of COSMO-CLM[2] benefiting from a new version of the atmospheric component and from an improved description of the partitioning between diffuse and direct light at the surface. We extend the work of Davin et al. (2011) by testing the two alternative LSMs in the context of two different versions of the atmospheric component, thus allowing to quantify the relative influence of land versus atmospheric processes. We furthermore aim at providing new insights into processes influencing land-atmosphere exchanges, namely by examining the role of diffuse/direct radiation partitioning at the surface. Observations indeed suggest that the ratio of diffuse to direct light influences plant photosynthesis, photosynthesis being enhanced under diffuse light conditions (Gu et al., 2003; Alton et al., 2007). This effect may have strong implications for the global carbon cycle (Mercado et al., 2009). On the other hand, evapotranspiration can also be affected by the light environment (Knohl and Baldocchi, 2008), since photosynthesis is tightly coupled to transpiration through stomatal control. Offline LSM simulations have suggested a possible impact of diffuse/direct radiation partitioning on land hydrology (Oliveira et al., 2011), but the possible feedbacks on climate have yet to be investigated. CLM3.5 explicitly distinguishes between diffuse and direct light in its canopy scheme and also represents the coupling between photosynthesis and transpiration, thus allowing to simulate the impact of light conditions on surface fluxes. Whereas our previous version of COSMO-CLM[2] assumed a fixed

**COSMO-CLM**[2]

E. L. Davin and
S. I. Seneviratne

diffuse to direct ratio for incoming shortwave radiation Davin et al. (2011), we test here the effect of allowing for variations in diffuse/direct ratio in the model.

## 2 Methods

### 2.1 COSMO-CLM²

COSMO-CLM² (Davin et al., 2011) couples the COSMO-CLM model (Rockel et al., 2008) to CLM3.5 (Oleson et al., 2004, 2008). COSMO-CLM is a non-hydrostatic RCM jointly used by the COnsortium for Small-scale Modelling (COSMO) and the Climate Limited-area Modelling Community (CLM-Community). CLM3.5 is a state of the art LSM representing the hydrological, biogeophysical and biogeochemical processes determining the exchanges of radiation, heat, water and carbon between the land and the atmosphere.

The native LSM in COSMO-CLM, TERRA_ML (Grasselt et al., 2008, and references therein), has been retained within COSMO-CLM² so that with the same atmospheric model either CLM3.5 or TERRA_ML can be used, allowing to quantify the influence of the LSM on the simulated climate. A description of the differences between CLM3.5 and TERRA_ML is provided by Davin et al. (2011).

Several options related to the dynamical core or the physical packages are available in the model. Here we use the second-order leapfrog scheme for the time integration. Vertical turbulent mixing is parametrized according to a level 2.5 closure using Turbulent Kinetic Energy (TKE) as a prognostic variable (Mellor and Yamada, 1974, 1982). For moist convection, the mass flux scheme of Tiedtke (1989) is used. CLM3.5 is used without carbon-nitrogen dynamics and ecosystem dynamics.

### 2.2 Summary of model improvements

New developments have been introduced in COSMO-CLM² compared to the previous version (Davin et al., 2011). First, the atmospheric component has been upgraded to a

newer version. Second, a modification of the coupling procedure regarding diffuse and direct fluxes from the atmospheric component to CLM3.5 has been introduced.

COSMO-CLM² has been initially developed based upon version 4.0 of COSMO-CLM (Davin et al., 2011). For this study, we upgraded to version 4.8 of COSMO-CLM. A number of modifications have been introduced between versions 4.0 and 4.8 some of which are reflected in Baldauf et al. (2011). Beside various bug corrections, the most notable improvement between these two versions relates to changes made to the Tiedtke cumulus convection scheme (Tiedtke, 1989). The newest version allows for a mixed water-ice phase when clouds condense (previously condensation occurred either as water or ice depending on air temperature) and an instantaneous evaporation of detrained convective clouds is not anymore assumed. Additionally, a number of other modifications apply to configurations not used in this study (e.g., Runge-Kutta dynamics, subgrid-scale orography, data assimilation) and therefore are not discussed here. Note also that TERRA_ML, the native LSM in COSMO-CLM, has not been modified between versions 4.0 and 4.8.

The coupling procedure regarding shortwave radiative fluxes has been revised to provide the LSM with both diffuse and direct beam fluxes from the atmospheric model. Note that this procedure is relevant only when CLM3.5 is used as the land component, since TERRA_ML does not make use of diffuse and direct fluxes in its calculations. CLM3.5 distinguishes between diffuse and direct radiation in its canopy radiative transfer scheme. An important assumption in this scheme is the two-leaf canopy approach in which the canopy is made up of a sunlit part (receiving both direct and diffuse light) and a shaded part (receiving only diffuse light). Photosynthesis and stomatal conductance are calculated separately for sunlit and shaded leaves and are thus affected by the amount of diffuse versus direct light (Thornton and Zimmermann, 2007). However, if the direct and diffuse radiation components are not explicitly provided, CLM3.5 uses the total incoming shortwave radiation and assumes a fixed 30/70 % (diffuse/direct) partitioning. This procedure is applied in the previous version of COSMO-CLM² (Davin et al., 2011). Here, we modified the coupling procedure in such a way that the surface

incoming diffuse and direct fluxes calculated by the $\delta$-two-stream atmospheric radiative transfer scheme in COSMO-CLM (Ritter and Geleyn, 1992) are provided explicitly to CLM3.5 instead of the total incoming shortwave flux.

## 2.3 Experiments

Five different experiments, summarized in Table 1, are analysed in this study. Experiments v4.0-TERRA_ML, v4.0-CLM3.5, v4.8-TERRA_ML and v4.8-CLM3.5 enable us to isolate the effect of the LSM (CLM3.5 versus TERRA_ML) on the simulated regional climate in the context of two different versions of the atmospheric component (4.0 versus 4.8). Experiment v4.8-CLM3.5-dif includes the modification to the treatment of diffuse and direct radiative fluxes. Therefore, comparing v4.8-CLM3.5-dif with v4.8-CLM3.5 (with fixed 30 % diffuse and 70 % direct) allows us to quantify the impact of introducing a spatially and temporally varying diffuse/direct partitioning in the model.

As in Davin et al. (2011), all five experiments use a horizontal resolution of 0.44° (~50 km) with 32 atmospheric levels in the vertical and a time step of 240s. The model domain encompasses the entire European continent, including parts of northern Africa and of Russia. The simulations cover the period from 1980 to 2006. ERA40 reanalysis data (Uppala et al., 2005) are used as lateral boundary conditions, except for the years 2002–2006 for which ECMWF operational forecast analyses are employed. $CO_2$, $CH_4$ and $N_2O$ concentrations are prescribed according to observed historical trends. The first 6 years are used as spin-up time and only the following years (1986–2006) are analysed.

## 2.4 Evaluation datasets

We use 2 m temperature, precipitation and total cloud cover from the Climate Research Unit (CRU) TS3.1 global 0.5° gridded dataset (Mitchell and Jones, 2005). The International Satellite Cloud Climatology Project (ISCCP) D2 dataset at 280 × 280 km resolution (Rossow and Schiffer, 1999) is also used as an alternative cloud cover dataset.

For the purpose of evaluating model performance at the sub-monthly (daily) time scale we also employ the E-OBS version 3.0 temperature dataset (Haylock et al., 2008).

The global 1° gridded dataset from the Global Soil Wetness Project (GSWP-2) (Dirmeyer et al., 2006) is also used in this study. This product is based on 13 LSMs which were all driven by the same observationally-based meteorological forcing for the period 1986–1995. We consider the multi-model mean from the GSWP-2 dataset as well as the multi-model standard deviation. We used ±2 × std as an estimate of the uncertainty range of the GSWP-2 dataset.

Observations of diffuse and direct shortwave radiation from three stations (Carpentras, Toravere and Payerne) within the BSRN (Baseline Surface Radiation Network) network (Ohmura et al., 1998) are used. The raw measurements were processed to derive monthly means using the procedure described in Roesch et al. (2011).

For the specific purpose of evaluating the sensitivity of evapotranspiration to light partitioning, we use data from the Hyytiälä (Finland) FLUXNET site (Suni et al., 2003). This site was chosen because it has the longest record of diffuse radiation measurements along with ET measurements compared to other European sites. The site is located at 181 m over an evergreen needleleaf forest (24.29° E 61.85° N). We use non-gap-filled radiation and evapotranspiration data from the period 2002–2005.

No corrections are applied to any of the datasets. For comparison, model outputs are interpolated onto the respective dataset grids and in the case of point-scale measurements (i.e., BSRN and FLUXNET) the model grid cell encompassing the site coordinates is considered. When results are presented over specific regions, the European sub-domains as defined in the PRUDENCE project are used (Christensen et al., 2007).

Full Screen / Esc

Printer-friendly Version

Interactive Discussion

## 3 Results

### 3.1 Overall influence of the LSM

#### 3.1.1 Radiation and clouds

Biases in radiation and cloud cover for experiments v4.0-TERRA_ML, v4.0-CLM3.5, v4.8-TERRA_ML and v4.8-CLM3.5 are shown in Figs. 1, 2 and 3 for the summer season. Davin et al. (2011) analysed simulations v4.0-TERRA_ML and v4.0-CLM3.5 and found an improvement in surface net shortwave radiation (shown here in Fig. 1a and c) when using CLM3.5 instead of TERRA_ML. Despite this improvement, a pronounced shortwave radiation underestimation still remains in the model. Results from experiments v4.8-TERRA_ML and v4.8-CLM3.5 indicate a positive influence of the new version of the atmospheric component (Fig. 1b and d), which further alleviates the shortwave radiation bias.

These successive improvements in surface net shortwave radiation can be traced back to the simulated cloud cover, since surface albedo does not vary strongly between the different experiments (not shown). Because of the inherent uncertainties in observed cloud cover, we use two different datasets to evaluate cloud cover biases in the model (Fig. 2 and 3). The amplitude of the inferred biases clearly depends on the reference dataset used, nevertheless the results remain qualitatively similar. Figures 2a and 3a show a large overestimation of total cloud cover in simulation v4.0-TERRA_ML, which explains the associated shortwave radiation underestimation. CLM3.5 as well as the new version of the atmospheric component both improve simulated fractional cloud cover, thus alleviating the preexisting shortwave radiation bias.

Davin et al. (2011) demonstrated that the effect of CLM3.5 on cloud cover is due to a better partitioning of latent versus sensible heat compared to TERRA_ML (with TERRA_ML overestimating latent heat relative to sensible heat). Concerning the effect of the atmospheric component, the improved cloud cover in the newest version can be traced back to the revised implementation of the Tiedtke convection scheme

**COSMO-CLM**[2]

E. L. Davin and
S. I. Seneviratne

as suggested by results from an additional experiment (v4.4-TERRA_ML). This experiment represents an intermediate model version in which the revisions to the Tiedtke scheme were first introduced. In terms of fractional cloud cover, experiment v4.4-TERRA_ML is strikingly similar to experiment v4.8-TERRA_ML and features the improved cloud cover behaviour compared to experiment v4.0-TERRA_ML (Fig. 4). This suggests that the revised Tiedtke scheme is the main factor explaining the improved fractional cloud cover in v4.8-TERRA_ML compared to v4.0-TERRA_ML. It is worth mentioning that the convection scheme itself does not affect directly the simulated cloudiness which is calculated diagnostically. Therefore, the improved cloud cover may be seen as an indirect consequence of the modified convection scheme, due to the fact that a modified convective activity influences the state of the atmosphere hence affecting cloudiness.

Combining the new version of the atmospheric component and CLM3.5 (Figs. 1d, 2d and 3d) gives the best performance for both shortwave radiation and cloud cover. Moreover, the LSM contribution to the bias reduction is of the same order as the contribution of the atmospheric component, highlighting the overall importance of the LSM for the quality of the simulation.

### 3.1.2 Temperature and precipitation

To obtain a quantitative estimate of the model performance in simulating 2 m temperature and precipitation, we use a RMSE-based score accounting for spatial, seasonal and interannual variability (Fig. 5). For each European sub-domain, the RMSE is calculated from the difference (model minus CRU) taken at each grid cell and for each month (monthly means) over the period 1986–2006.

For most regions, the best scores are reached with experiments v4.8-CLM3.5 including CLM3.5 instead of TERRA_ML and the new version of the atmospheric component. The positive influence of CLM3.5 is particularly important for temperature and less marked for precipitation. The effect on precipitation is dominated by the atmospheric component, whereas for temperature the LSM has the most impact.

## 3.2 Role of diffuse/direct radiation partitioning

We focus now on the influence of diffuse/direct radiation partitioning on surface fluxes and climate. In experiment v4.8-CLM3.5-dif, the ratio of diffuse to direct light as seen by CLM3.5 is allowed to vary spatially and temporally. We compare v4.8-CLM3.5-dif to experiment v4.8-CLM3.5 in which CLM3.5 instead assumes a constant diffuse to direct ratio.

In the following we first evaluate the ability of the model to realistically represent the partitioning of diffuse versus direct light (through the radiative transfer scheme of the atmospheric component). Then, we examine the sensitivity of CLM3.5 to light partitioning and compare it to observations. Finally, we analyse the effect of these processes on the mean climate and climate variability in the model.

### 3.2.1 Evaluation of diffuse/direct partitioning

Figure 6 shows time series of diffuse fraction (ratio of incoming diffuse light to total incoming shortwave radiation at the surface) for three different European sites. Observations are from the BSRN network and modeled values correspond to the radiation partitioning as seen by CLM3.5. In the case of experiment v4.8-CLM3.5, this partitioning is set to a constant value of 30 % diffuse radiation whereas in experiment v4.8-CLM3.5-dif the radiation partitioning comes as an input from the atmospheric component (through provision of the diffuse and direct radiation incoming fluxes separately instead of just total incoming shortwave radiation as in experiment v4.8-CLM3.5).

For all 3 sites, the 30 % diffuse radiation partitioning appears to be on average too low compared to observations and furthermore it does not account for the large seasonal and interannual variations seen in observations. On the other hand, the partitioning in experiment v4.8-CLM3.5-dif is in good agreement with observations. In particular the seasonal cycle (more diffuse light in winter than in summer) is well represented and some features of the interannual variability are also captured.

E. L. Davin and
S. I. Seneviratne

Title Page

Abstract | Introduction

Conclusions | References

Tables | Figures

◄ | ►

◄ | ►

Back | Close

Full Screen / Esc

Printer-friendly Version

Interactive Discussion

These results indicate that providing separately the incoming diffuse and direct components from the atmospheric component to CLM3.5 represents a real improvement compared to the default fixed partitioning used in CLM3.5.

### 3.2.2   Evapotranspiration response to diffuse/direct partitioning

Observations suggest that plants tend to be photosynthetically more active under diffuse light conditions (Gu et al., 2003; Alton et al., 2007). Considering the tight coupling between photosynthesis and transpiration and the fact that transpiration is the main contributor to land evapotranspiration (Dirmeyer et al., 2006), light partitioning is also expected to affect water fluxes (Oliveira et al., 2011).

We analyse observational data from a flux measurement site to examine the sensitivity of latent heat to diffuse versus direct light conditions (Fig. 7). The latent heat flux is plotted against incoming shortwave radiation, showing the increase in latent heat with increasing radiation. We further discriminate between diffuse and direct conditions based on the observed diffuse fraction. We choose a threshold of diffuse fraction above 65 % and below 35 % to represent diffuse and direct conditions, respectively.

For a given amount of incoming radiation, the latent heat flux tends to be larger under diffuse compared to direct conditions, a phenomenon that has already been documented at an other site (Knohl and Baldocchi, 2008). This observed behaviour is qualitatively and quantitatively well reproduced by the model in experiment v4.8-CLM3.5-dif. Although this comparison is restricted to a single site, this gives some confidence that canopy processes are realistically represented in CLM3.5 and that the sensitivity of evapotranspiration to variations in light partitioning is relatively well captured.

### 3.2.3   Effect on the mean climate state

Figure 8 displays differences between experiments v4.8-CLM3.5 and v4.8-CLM3.5-dif for various surface variables. Since no significant differences are found in winter (not

shown), we analyse only the summer season. Diffuse fraction is on average higher in experiment v4.8-CLM3.5-dif compared to v4.8-CLM3.5 (Fig. 8a). As a consequence, both photosynthesis and transpiration are increased in experiment v4.8-CLM3.5-dif (Fig. 8b and c). The relative change in photosynthesis is larger than for transpiration
5 implying a rise in plant's water use efficiency with increasing diffuse light. This result is in line with earlier observational evidences (Knohl and Baldocchi, 2008). The change in total evapotranspiration (Fig. 8d) is somewhat less pronounced than the transpiration change due to a concurrent decrease in bare soil evaporation (not shown), but it is in line with the observational evidence of an enhancement of evapotranspiration under
10 diffuse light conditions (Sect. 3.2.2).

The effect on surface temperature (Fig. 9) is consistent with the overall increase in evapotranspiration leading to a surface cooling. This cooling brings experiment v4.8-CLM3.5-dif closer to observations by reducing the warm bias present in experiment v4.8-CLM3.5.

15 ## 3.2.4  Implications for climate variability

Variations in the diffuse/direct ratio at the surface can influence evapotranspiration and the surface energy balance and can thus induce variations in temperature and other climate variables. By accounting for this process, experiment v4.8-CLM3.5-dif incorporates an additional source of climate variability compared to experiment v4.8-CLM3.5.
20 To assess the added value of taking this process into account, we analyse the model skills in simulating 2 m temperature variability at the monthly and daily time scales.

Based on time series aggregated over 8 sub-domains and focusing on the summer season, we calculate the squared correlations ($R^2$) between model and observations, using either monthly or daily averages (Table 2). $R^2$ values are found to be higher
25 in experiment v4.8-CLM3.5-dif for all regions (except for BI where there is no change in the $R^2$ value between v4.8-CLM3.5 and v4.8-CLM3.5-dif). $R^2$ values are overall higher at the monthly time scale in both experiments, but the increase in $R^2$ values in experiment v4.8-CLM3.5-dif, which ranges between 0–3 %, is of similar magnitude for

both monthly and daily time scales. We note that a similar analysis for precipitation (not shown) leads to inconclusive results.

These results indicate that accounting for variations in diffuse/direct ratio at the surface consistently improves the model performance with respect to summer temperature variability. This effect remains quantitatively limited. Comparing experiments v4.8-CLM3.5 and v4.8-CLM3.5-dif we find that this process may explain up to 3 % of the summer temperature variability at the monthly and daily time scales.

## 4   Conclusions

By testing two alternative LSMs within a RCM, this study quantitatively addresses the role of land processes in simulating regional climate over Europe. We use the COSMO-CLM RCM either with its native LSM (TERRA_ML) or coupled to the more advanced CLM3.5. In a previous study based on COSMO-CLM version 4.0, Davin et al. (2011) found improvements in the simulated climate over Europe when using CLM3.5, owing to more realistic surface fluxes in CLM3.5 compared to TERRA_ML. Here, we present evidences of the robustness of this conclusion by showing that the positive effect of CLM3.5 remains true in the context of a new improved version of COSMO-CLM (version 4.8). Moreover, we show that the influence of the LSM on the simulated climate can be typically as large as that from the atmospheric component, at least in summer. This is particularly the case for near-surface temperature, while precipitation is more affected by changes in the atmospheric component. Overall, the best model performance is achieved when the more advanced LSM (CLM3.5 instead of TERRA_ML) is combined with the improved version of the atmospheric component (v4.8 instead v4.0). In this case, the substantial underestimation of surface net shortwave radiation which was noted as a remaining deficiency in the previous version of COSMO-CLM[2] (Davin et al., 2011) is largely alleviated. One central aspect allowing for the noted improvements is the simulated cloudiness, which is positively affected on one hand by the better partitioning of surface fluxes in CLM3.5 and on the other hand by the revised convection scheme included in COSMO-CLM version 4.8.

We furthermore explore the impact of diffuse/direct radiation partitioning on surface fluxes and climate and its potential added value in regional simulations. An experiment where the diffuse and direct radiation components are explicitly provided to CLM3.5 (instead of a fixed diffuse/direct ratio) is performed. Comparison with observations
5 shows that the model, through its atmospheric radiative transfer scheme, realistically captures seasonal and interannual variations in diffuse/direct radiation partitioning at the surface. Moreover, the increase in ET under diffuse light conditions seen in eddy-flux measurements is also captured by the land model. When taking explicitly into account variations in diffuse/direct light partitioning at the surface in the model, a sig-
10 nificant improvement in simulated summer temperature variability both at the monthly and the daily time scales is noted. A small fraction (up to 3%) of the overall variability in surface temperature can be attributed to diffuse/direct light variations in our experiments. Our experiments also show that the average level of diffuse radiation can strongly impact the partitioning between latent and sensible heat with consequence on
15 surface temperature. It is worth mentioning that canopy processes in CLM, in particular radiative transfer in the canopy, have been recently revised (Bonan et al., 2011). Although this version is not yet available, a future reassessment of our conclusions using these new developments may help quantifying modelling uncertainties attached to these processes.

Printer-friendly Version

Interactive Discussion

# References

Alton, P. B., North, P. R., and Los, S. O.: The impact of diffuse sunlight on canopy light-use efficiency, gross photosynthetic product and net ecosystem exchange in three forest biomes, Global Change Biol., 13, 776–787, doi:10.1111/j.1365-2486.2007.01316.x, 2007. 11604, 11612

Arneth, A., Harrison, S. P., Zaehle, S., Tsigaridis, K., Menon, S., Bartlein, P. J., Feichter, J., Korhola, A., Kulmala, M., O'Donnell, D., Schurgers, G., Sorvari, S., and Vesala, T.: Terrestrial biogeochemical feedbacks in the climate system, Nat. Geosci., 3, 525–532, doi:10.1038/ngeo905, 2010. 11602

Baldauf, M., Seifert, A., Frstner, J., Majewski, D., Raschendorfer, M., and Reinhardt, T.: Operational convective-scale numerical weather prediction with the COSMO model: description and sensitivities, Mon. Weather Rev., 139, 3887–3905, doi:10.1175/MWR-D-10-05013.1, 2011. 11606

Bonan, G. B.: Forests and climate change: Forcings, feedbacks, and the climate benefits of forests, Science, 320, 1444–1449, doi:10.1126/science.1155121, 2008. 11602

Bonan, G. B., Lawrence, P. J., Oleson, K. W., Levis, S., Jung, M., Reichstein, M., Lawrence, D. M., and Swenson, S. C.: Improving canopy processes in the Community Land Model version 4 (CLM4) using global flux fields empirically inferred from FLUXNET data, J. Geophys. Res., 116, G02014, doi:10.1029/2010JG001593, 2011. 11615

Christensen, J. H., Carter, T. R., Rummukainen, M., and Amanatidis, G.: Evaluating the performance and utility of regional climate models: the PRUDENCE project, Clim. Change, 81, 1–6, doi:10.1007/s10584-006-9211-6, 2007. 11608

Davin, E. L., Stoeckli, R., Jaeger, E. B., Levis, S., and Seneviratne, S. I.: COSMO-CLM[2]: a new version of the COSMO-CLM model coupled to the Community Land Model, Clim. Dyn., 37, 1889–1907, doi:10.1007/s00382-011-1019-z, 2011. 11604, 11605, 11606, 11607, 11609, 11614, 11620

Denning, A., Nicholls, M., Prihodko, L., Baker, I., Vidale, P., Davis, K., and Bakwin, P.: Simulated variations in atmospheric $CO_2$ over a Wisconsin forest using a coupled ecosystem-atmosphere model, Global Change Biol., 9, 1241–1250, 2003. 11603

Dirmeyer, P. A., Gao, X., Zhao, M., Guo, Z., Oki, T., and Hanasaki, N.: GSWP-2 – Multimodel anlysis and implications for our perception of the land surface, Bull. Amer. Meteorol. Soc., 87, 1381-1397, doi:10.1175/BAMS-87-10-1381, 2006. 11608, 11612

Title Page

Abstract | Introduction

Conclusions | References

Tables | Figures

◄◄ | ►►

◄ | ►

Back | Close

Full Screen / Esc

Printer-friendly Version

Interactive Discussion

Friedlingstein, P., Cox, P., Betts, R., Bopp, L., Von Bloh, W., Brovkin, V., Cadule, P., Doney, S., Eby, M., Fung, I., Bala, G., John, J., Jones, C., Joos, F., Kato, T., Kawamiya, M., Knorr, W., Lindsay, K., Matthews, H. D., Raddatz, T., Rayner, P., Reick, C., Roeckner, E., Schnitzler, K. G., Schnur, R., Strassmann, K., Weaver, A. J., Yoshikawa, C., and Zeng, N.: Climate-carbon cycle feedback analysis: Results from the (CMIP)-M-4 model intercomparison, J. Clim., 19, 3337–3353, 2006. 11603

Giorgi, F.: Regional climate modeling: Status and perspectives, J. Phys. IV, 139, 101–118, doi:10.1051/jp4:2006139008, 2006. 11603

Grasselt, R., Schuettemeyer, D., Warrach-Sagi, K., Ament, F., and Simmer, C.: Validation of TERRA-ML with discharge measurements, Meteorol. Z., 17, 763–773, doi:10.1127/0941-2948/2008/0334, 2008. 11605

Gu, L., Baldocchi, D., Wofsy, S., Munger, J., Michalsky, J., Urbanski, S., and Boden, T.: Response of a deciduous forest to the Mount Pinatubo eruption: Enhanced photosynthesis, Science, 299, 2035–2038, 2003. 11604, 11612

Haylock, M. R., Hofstra, N., Tank, A. M. G. K., Klok, E. J., Jones, P. D., and New, M.: A European daily high-resolution gridded data set of surface temperature and precipitation for 1950-2006, J. Geophys. Res., 113, doi:10.1029/2008JD010201, 2008. 11608

Knohl, A. and Baldocchi, D. D.: Effects of diffuse radiation on canopy gas exchange processes in a forest ecosystem, J. Geophys. Res., 113, doi:10.1029/2007JG000663, 2008. 11604, 11612, 11613

Lu, L., Pielke, R., Liston, G., Parton, W., Ojima, D., and Hartman, M.: Implementation of a two-way interactive atmospheric and ecological model and its application to the central United States, J. Clim., 14, 900–919, 2001. 11603

Manabe, S.: Climate and Ocean Circulation.I. Atmospheric Circulation and Hydrology of Earths Surface, Mon. Weather Rev., 97, 739–774, 1969. 11603

Mellor, G. L. and Yamada, T.: Hierarchy of turbulence closure models for planetary boundary-layers, J. Atmos. Sci., 31, 1791–1806, 1974. 11605

Mellor, G. L. and Yamada, T.: Development of a turbulence closure-model for geophysical fluid problems, Rev. Geophys., 20, 851–875, 1982. 11605

Mercado, L. M., Bellouin, N., Sitch, S., Boucher, O., Huntingford, C., Wild, M., and Cox, P. M.: Impact of changes in diffuse radiation on the global land carbon sink, Nature, 458, 1014–1017, doi:10.1038/nature07949, 2009. 11604

Mitchell, T. and Jones, P.: An improved method of constructing a database of monthly cli-

**COSMO-CLM$^2$**

E. L. Davin and
S. I. Seneviratne

| | |
|---|---|
| Title Page | |
| Abstract | Introduction |
| Conclusions | References |
| Tables | Figures |
| ◄◄ | ►► |
| ◄ | ► |
| Back | Close |
| Full Screen / Esc | |

Printer-friendly Version

Interactive Discussion

mate observations and associated high-resolution grids, Int. J. Climatol., 25, 693–712, doi:10.1002/joc.1181, 2005. 11607

Ohmura, A., Dutton, E., Forgan, B., Frohlich, C., Gilgen, H., Hegner, H., Heimo, A., Konig-Langlo, G., McArthur, B., Muller, G., Philipona, R., Pinker, R., Whitlock, C., Dehne, K., and Wild, M.: Baseline Surface Radiation Network (BSRN/WCRP): New precision radiometry for climate research, Bull. Amer. Meteorol. Soc., 79, 2115–2136, doi:10.1175/1520-0477(1998)079¡2115:BSRNBW¿2.0.CO;2, 1998. 11608

Oleson, K. W., Dai, Y., Bonan, G. B., Bosilovich, M., Dickinson, R. E., Dirmeyer, P., Hoffman, F., Houser, P., Levis, S., Niu, G. Y., Thornton, P. E., Vertenstein, M., Yang, Z. L., and Zeng, X.: Technical description of the Community Land Model (CLM), NCAR Tech. Note NCAR/TN-461+STR, Natl. Cent. for Atmos. Res., Boulder, Colo., 2004. 11605

Oleson, K. W., Niu, G. Y., Yang, Z. L., Lawrence, D. M., Thornton, P. E., Lawrence, P. J., Stoeckli, R., Dickinson, R. E., Bonan, G. B., Levis, S., Dai, A., and Qian, T.: Improvements to the Community Land Model and their impact on the hydrological cycle, J. Geophys. Res., 113, G01021, doi:10.1029/2007JG000563, 2008. 11605

Oliveira, P. J. C., Davin, E. L., Levis, S., and Seneviratne, S. I.: Vegetation-mediated impacts of trends in global radiation on land hydrology: a global sensitivity study, Global Change Biol., 17, 3453–3467, doi:10.1111/j.1365-2486.2011.02506.x, 2011. 11604, 11612

Ritter, B. and Geleyn, J.: A comprehensive radiation scheme for numerical weather prediction models with potential applications in climate simulations, Mon. Weather Rev., 120, 303–325, 1992. 11607

Rockel, B., Will, A., and Hense, A., in: Special Issue: Regional Climate Modelling With COSMO-CLM (CCLM), vol. 17 of 4, Meteorol. Z., 2008. 11605

Roesch, A., Wild, M., Ohmura, A., Dutton, E. G., Long, C. N., and Zhang, T.: Assessment of BSRN radiation records for the computation of monthly means, Atmos. Meas. Tech., 4, 339–354, doi:10.5194/amt-4-339-2011, 2011. 11608

Rossow, W. and Schiffer, R.: Advances in understanding clouds from ISCCP, Bull. Amer. Meteorol. Soc., 80, 2261–2287, 1999. 11607

Seneviratne, S. I., Corti, T., Davin, E. L., Hirschi, M., Jaeger, E. B., Lehner, I., Orlowsky, B., and Teuling, A. J.: Investigating soil moisture-climate interactions in a changing climate: A review, Earth-Sci. Rev., 99, 125–161, doi:10.1016/j.earscirev.2010.02.004, 2010. 11602

Steiner, A. L., Pal, J. S., Rauscher, S. A., Bell, J. L., Diffenbaugh, N. S., Boone, A., Sloan, L. C., and Giorgi, F.: Land surface coupling in regional climate simulations of the West African

monsoon, Clim. Dyn., 33, 869–892, doi:10.1007/s00382-009-0543-6, 2009. 11603

Subin, Z. M., Riley, W. J., Jin, J., Christianson, D. S., Torn, M. S., and Kueppers, L. M.: Ecosystem Feedbacks to Climate Change in California: Development, Testing, and Analysis Using a Coupled Regional Atmosphere and Land Surface Model (WRF3-CLM3.5), Earth Interact., 15, 1–38, doi:10.1175/2010EI331.1, 2011. 11603

Suni, T., Rinne, J., Reissell, A., Altimir, N., Keronen, P., Rannik, U., Dal Maso, M., Kulmala, M., and Vesala, T.: Long-term measurements of surface fluxes above a Scots pine forest in Hyytiala, southern Finland, 1996-2001, Boreal Environ. Res., 8, 287–301, 2003. 11608

Thornton, P. E. and Zimmermann, N. E.: An improved canopy integration scheme for a land surface model with prognostic canopy structure, J. Clim., 20, 3902–3923, doi:10.1175/JCLI4222.1, 2007. 11606

Tiedtke, M.: a comprehensive mass flux scheme for cumulus parameterization in large-scale models, Mon. Weather Rev., 117, 1779–1800, 1989. 11605, 11606

Uppala, S., Kallberg, P., Simmons, A., Andrae, U., Bechtold, V., Fiorino, M., Gibson, J., Haseler, J., Hernandez, A., Kelly, G., Li, X., Onogi, K., Saarinen, S., Sokka, N., Allan, R., Andersson, E., Arpe, K., Balmaseda, M., Beljaars, A., Van De Berg, L., Bidlot, J., Bormann, N., Caires, S., Chevallier, F., Dethof, A., Dragosavac, M., Fisher, M., Fuentes, M., Hagemann, S., Holm, E., Hoskins, B., Isaksen, L., Janssen, P., Jenne, R., McNally, A., Mahfouf, J., Morcrette, J., Rayner, N., Saunders, R., Simon, P., Sterl, A., Trenberth, K., Untch, A., Vasiljevic, D., Viterbo, P., and Woollen, J.: The ERA-40 re-analysis, Quart. J. Roy. Met. Soc., 131, 2961–3012, doi:10.1256/qj.04.176, 2005. 11607

Wang, J.-W., Denning, A. S., Lu, L., Baker, I. T., Corbin, K. D., and Davis, K. J.: Observations and simulations of synoptic, regional, and local variations in atmospheric CO2, J. Geophys. Res., 112, D04108, doi:10.1029/2006JD007410, 2007. 11603

Winter, J. M., Pal, J. S., and Eltahir, E. A. B.: Coupling of Integrated Biosphere Simulator to Regional Climate Model Version 3, J. Clim., 22, 2743–2757, doi:10.1175/2008JCLI2541.1, 2009. 11603

Title Page

Abstract | Introduction

Conclusions | References

Tables | Figures

◄◄ | ►►

◄ | ►

Back | Close

Full Screen / Esc

Printer-friendly Version

Interactive Discussion

**Table 1.** Summary of the different experiments analysed in this study.

| Experiment name | Atmospheric component | LSM | Other comments |
|---|---|---|---|
| v4.0-TERRA_ML | 4.0 | TERRA_ML | same as experiment COSMO-CLM in Davin et al. (2011) |
| v4.0-CLM3.5 | 4.0 | CLM3.5 | same as experiment COSMO-CLM[2] in Davin et al. (2011) |
| v4.8-TERRA_ML | 4.8 | TERRA_ML | |
| v4.8-CLM3.5 | 4.8 | CLM3.5 | |
| v4.8-CLM3.5-dif | 4.8 | CLM3.5 | same as experiment v4.8-CLM3.5 except that downward diffuse and direct components are explicitly passed to CLM3.5 instead of assuming a fixed diffuse/direct partitioning |

**Table 2.** Squared correlation ($R^2$) between modeled and observed (E-OBS) 2 m temperature. Time series are domain-averaged over eight different regions as defined in Fig. 5. Correlations are based either on monthly or daily means in both cases considering only data between June and August.

| Experiment | sub-domains | | | | | | | |
|---|---|---|---|---|---|---|---|---|
| | BI | IP | FR | ME | SC | AL | MD | EA |
| monthly time scale | | | | | | | | |
| v4.8-CLM3.5 | 0.92 | 0.90 | 0.87 | 0.89 | 0.88 | 0.85 | 0.82 | 0.71 |
| v4.8-CLM3.5-dif | 0.92 | 0.91 | 0.88 | 0.90 | 0.91 | 0.88 | 0.85 | 0.74 |
| daily time scale | | | | | | | | |
| v4.8-CLM3.5 | 0.79 | 0.86 | 0.82 | 0.82 | 0.72 | 0.80 | 0.72 | 0.73 |
| v4.8-CLM3.5-dif | 0.79 | 0.87 | 0.84 | 0.83 | 0.74 | 0.82 | 0.74 | 0.75 |
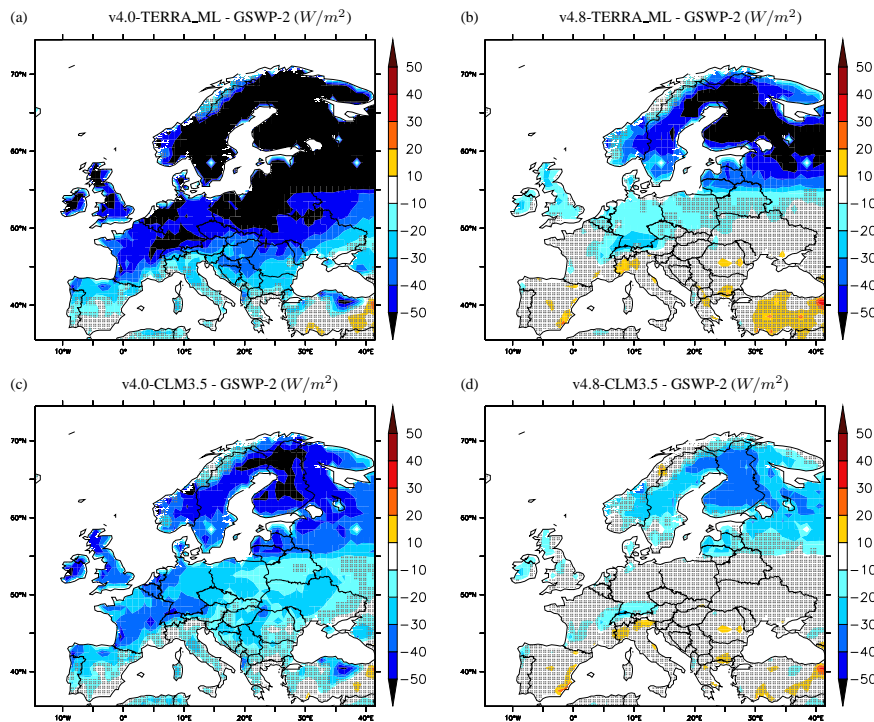
**Fig. 1.** Summer (JJA) mean net shortwave radiation bias (model minus GSWP-2) for the different experiments. The considered time period is 1986–1995 and areas where the model bias is within the GSWP-2 uncertainty range are indicated with grey shading.
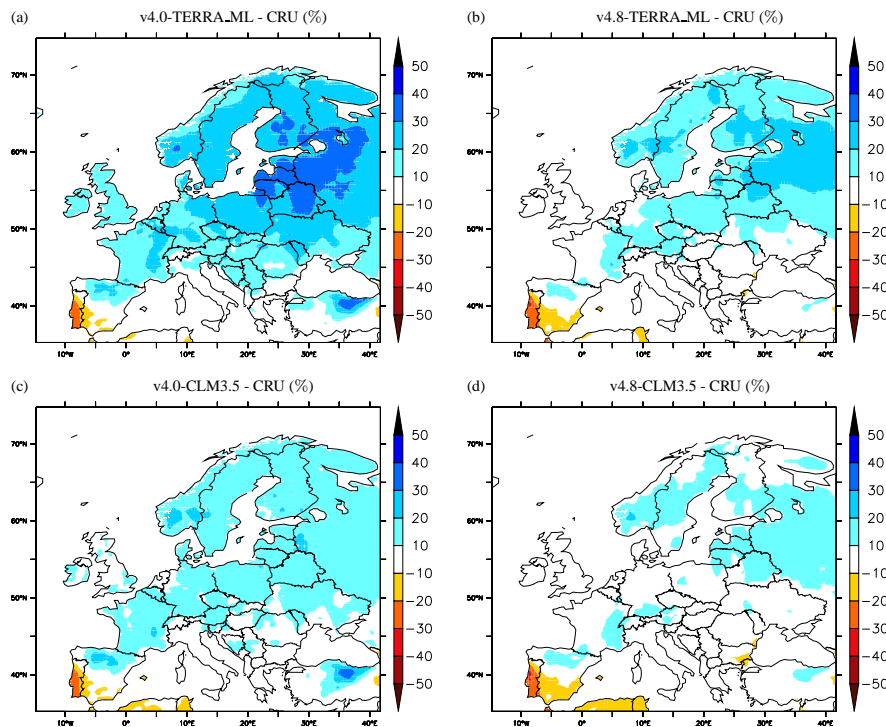
**Fig. 2.** Summer (JJA) mean cloud cover bias (model minus CRU) for the different experiments. The considered time period is 1986–1995.
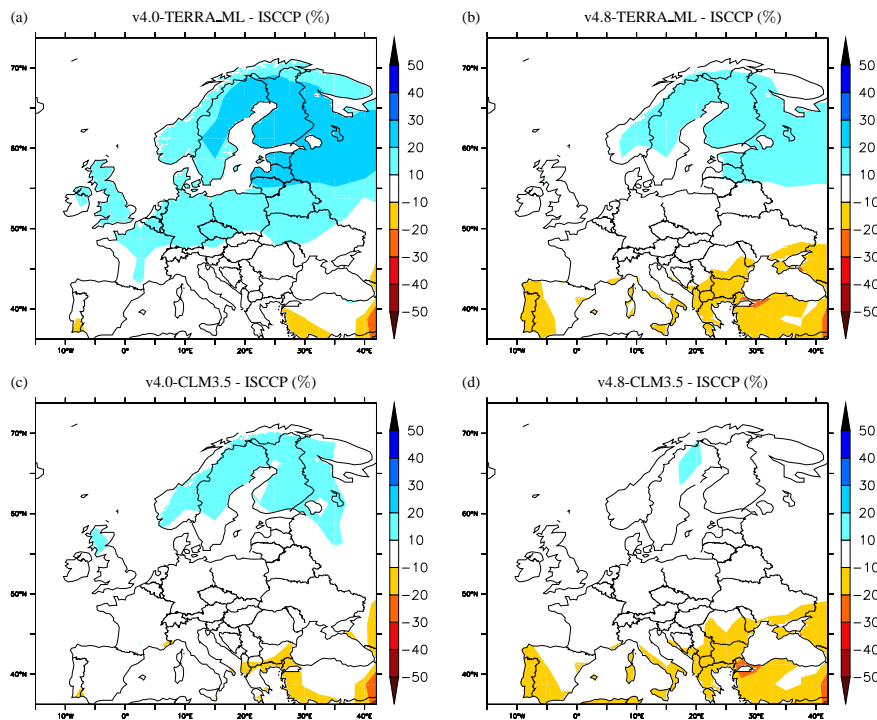
**Fig. 3.** Same as Fig. 2 but in reference to ISCCP instead of CRU.

E. L. Davin and
S. I. Seneviratne

Full Screen / Esc
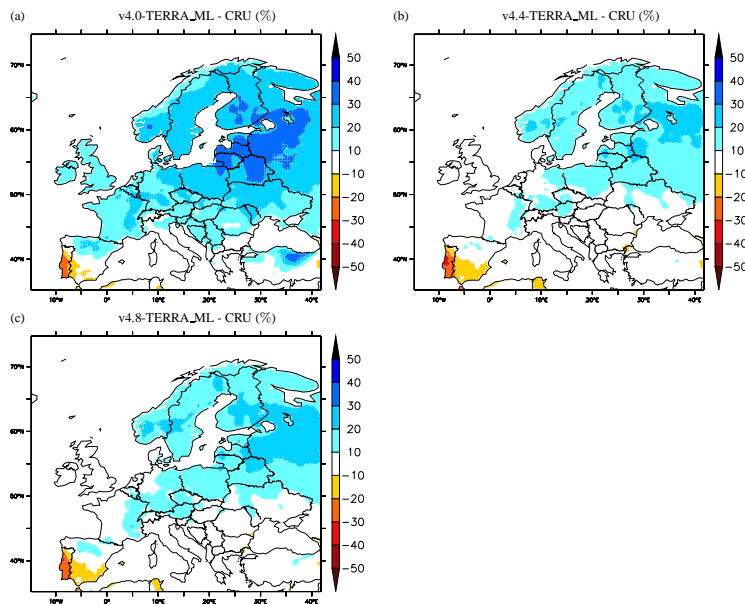
**Fig. 4.** Summer (JJA) mean cloud cover bias (model minus CRU) for experiments v4.0-TERRA_ML, v4.4-TERRA_ML and v4.8-TERRA_ML. The considered time period is 1986–1995.
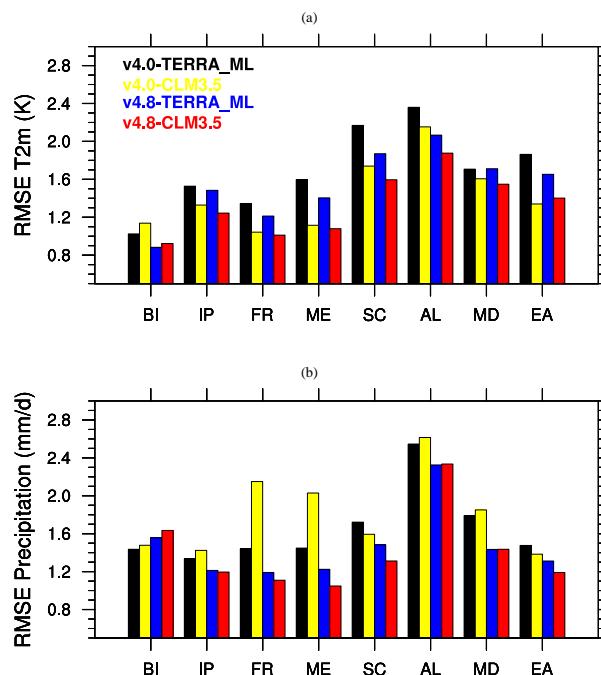
**Fig. 5.** Model performance for **(a)** 2 m temperature and **(b)** precipitation, for the different model experiments. BI: British Isles; IP: Iberian Peninsula; FR: France; ME: Mid-Europe; SC: Scandinavia; AL: Alps; MD: Mediterranean; EA: Eastern Europe. The considered score is the RMSE calculated from the differences (model minus CRU) taken at each grid cell and for each month (monthly means) over the time period 1986–2006.

Full Screen / Esc

Printer-friendly Version

Interactive Discussion
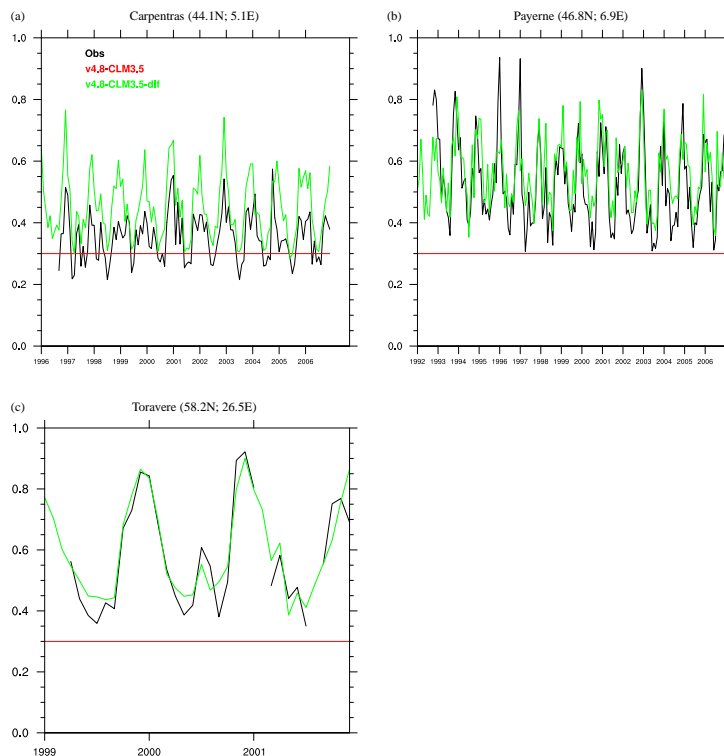


**Fig. 6.** Time series of diffuse light fraction (monthly means) at three different BSRN sites.
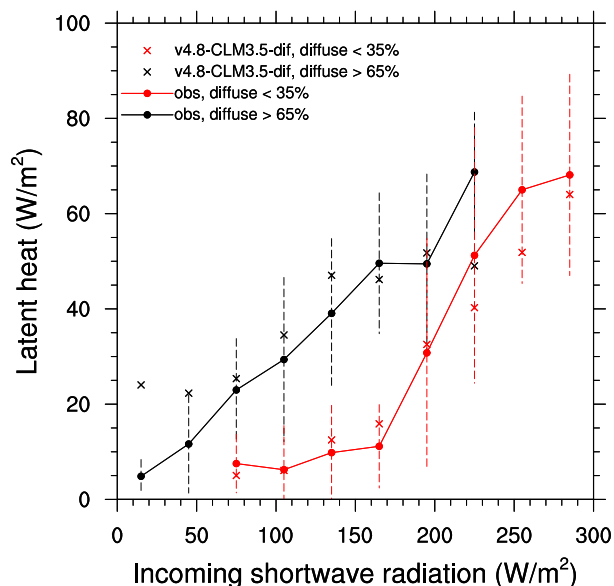
**Fig. 7.** Sensitivity of latent heat to total incoming shortwave radiation for predominantly diffuse light conditions (black) and predominantly direct light conditions (red) at the Hyytiälä site. The underlying data are daily means over the period 2002–2005 restricted to spring and summer (growing season). Diffuse and direct conditions are defined as diffuse light fraction above 65 % and below 35 %, respectivelly. The points represent the mean latent heat for specific radiation bins. For the observations the standard deviation is also shown.
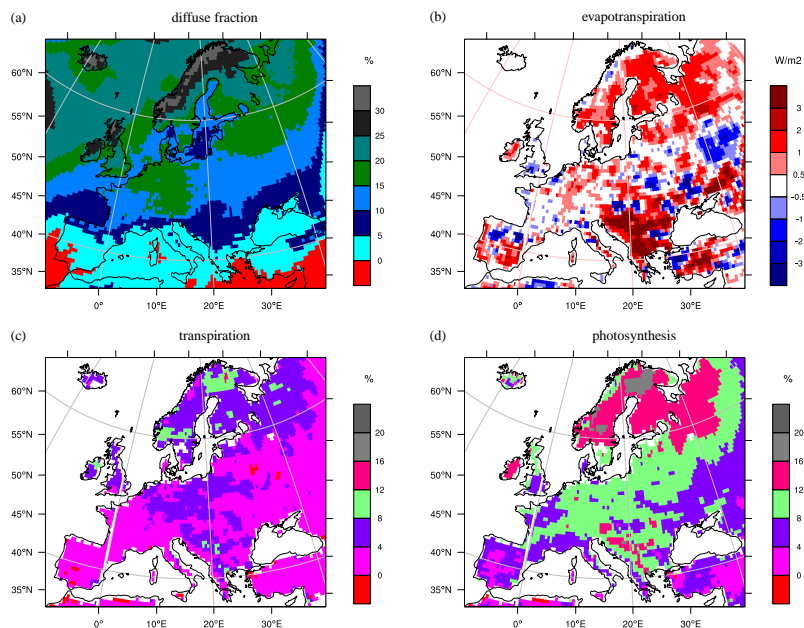
**Fig. 8.** Summer (JJA) mean change in diffuse fraction, photosynthesis, transpiration and evapo-transpiration (v4.8-CLM3.5-dif minus v4.8-CLM3.5). The considered time period is 1986–2006.
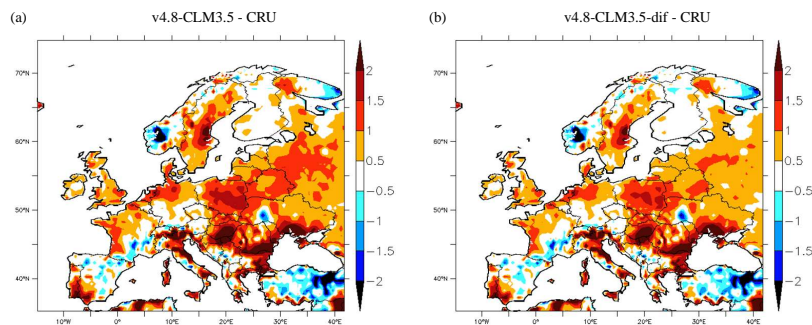
**Fig. 9.** Summer (JJA) mean 2 m temperature bias (model minus CRU) for experiments v4.8-CLM3.5 and v4.8-CLM3.5-dif. The considered time period is 1986–2006.